Pergamon

Geochimica et Cosmochimica Acta, Vol. 64, No. 6, pp. 1095–1102, 2000

0016-7037/00 $20.00 + .00

PII S0016-7037(99)00383-X

Modeling of trace element fractionation during non-modal dynamic melting with linear variations in mineral/melt distribution coefficients

HAIBO ZOU*

Department of Earth and Space Sciences, University of California at Los Angeles, Los Angeles, CA 90095-1567, USA

(*Received June* 10, 1999; *accepted in revised form October* 7, 1999)

Abstract—Recently significant advancement has been made in the modeling of trace element fractionation during dynamic melting. Some of the theoretical treatments that have contributed to the advancement took into account the variations in source mineral proportions, but all of them assumed constant mineral/melt distribution coefficients. This study introduces linear variations of mineral/melt distribution coefficients into the dynamic melting model. Analytical solutions are provided for this model with variations not only in source mineral proportions but also in mineral/melt distribution coefficients. Applications of these equations to mantle melting to incorporate variable clinopyroxene/melt distribution coefficients during initial stages of melting can reduce the required involvement of garnet for the generation of mid-ocean ridge basalts. The effects of variable mineral/melt distribution coefficients on trace element fractionation need to be carefully assessed in trace element studies of the petrogenesis of igneous rocks and their melt inclusions. *Copyright © 2000 Elsevier Science Ltd*

1. INTRODUCTION

Equations that describe trace element fractionation during mantle melting are fundamental to the interpretation of chemical compositions of igneous rocks. A recent significant achievement in trace element modeling is the development of the dynamic melting model (Langmuir et al., 1977; Maaløe, 1982; McKenzie, 1985; Maaløe and Johnson, 1986; Williams and Gill, 1989; Pedersen and Hertogen, 1990; Sobolev and Shimizu, 1992; Ozawa and Shimizu, 1995; Albarède, 1995; Zou and Zindler, 1996; Zou, 1998). In the context of dynamic melting, when the degree of partial melting is less than the critical mass porosity, there is no melt extraction; and when the degree of partial melting is greater than the critical mass porosity, any infinitesimal excess melt is extracted from the residue. After melt extraction begins, there are three subsystems in an open system: the residual solid undergoing partial melting, the interstitial melt which remains in equilibrium with the residual solid, and the extracted melt that is formed from continuous extraction of the residual melt and isolated from the residual solid. Detailed sketches illustrating the dynamic melting model can be found in Figure 3 in McKenzie (1985), Figure 1 in Williams and Gill (1989), and Figures 1 and 3 in Zou (1998). This model is supported by observations from ultra-depleted melt inclusions in olivine grains (Sobolev and Shimizu, 1993; Gurenko and Chaussidon, 1995; Shimizu, 1998), uranium-series disequilibrium data of young basalts (e.g., Beattie, 1993; Chabaux and Allègre, 1994), and extremely depleted clinopyroxenes from abyssal peridotites (Johnson, et al., 1990) and cumulates (Ross and Elthon, 1993).

During partial melting, the bulk distribution coefficient for the solid source is defined by Shaw (1970) as

$$D_{s/f} = \Sigma x^i K^i \quad (1)$$

where x^i is the mass fraction of phase i in the solid, and K^i is the mineral/melt distribution coefficient of phase i (a complete list of symbols is available in Appendix A for easy reference). Even though some studies (Pedersen and Hertogen, 1990; Sobolev and Shimizu 1992; Ozawa and Shimizu, 1995; Zou, 1998) have considered the variation of x^i during melting, constant K^i was assumed in all previous theoretical treatments of dynamic melting. However, it has been demonstrated that mineral/melt distribution coefficients are functions of temperature, pressure, and bulk composition of solid and liquid phases (e.g., Baker et al., 1995; Blundy et al., 1998). As the accuracy of estimated distribution coefficients is getting better, it is useful to consider the effects of variable distribution coefficients. The main aim of this paper is to introduce linear variations of mineral/melt distribution coefficients into the dynamic melting model so as to derive the equations that take into account not only changes in mineral proportions but also variations in mineral/melt distribution coefficients. In addition, the effects of variations in mineral/melt distribution coefficients on trace element fractionation are evaluated and the geochemical applications of these equations are also discussed.

2. DERIVATION

In a way similar to that of Shaw (1970) for perfect fractional melting, we define M_0 to be the initial mass and M_L the mass of the extracted melt. Thus (M_0-M_L) is the mass of the total residue, which includes the residual melt and the residual solid in dynamic melting. Similarly, m_0 is defined to be the mass of the element in question in the initial solid and m_L the mass of the element in the extracted melt, and (m_0-m_L) is the mass of the element in the total residue. Therefore, the concentration of the element of the last increment of the extracted melt is $dm_L/dM_L$and the concentration of the element in the total residue is $(m_0-m_L)/(M_0-M_L)$. Let D_{eff} be the effective distribution coefficient of the element, which is the ratio of the concentration of the element in the total residue over the

*Author to whom correspondence should be addressed (hzou@ess.ucla.edu).

concentration of the element in the last increment of the extracted melt, we have

$$D_{eff} = \left(\frac{m_0 - m_L}{M_0 - M_L}\right) \Big/ \left(\frac{dm_L}{dM_L}\right) \quad (2)$$

We define the mass fraction of the extracted melt relative to the initial source as $X = M_L/M_0$, the source concentration of the element as $C_O = m_0/M_0$, and the concentration in the extracted melt as $\overline{C_L} = m_L/M_L$. With the above definitions, Eqn. 2 may be written as

$$\frac{d(\overline{C_L}\, X)}{C_0 - \overline{C_L}\, X} = \frac{1}{D_{eff}} \frac{dX}{1 - X} \quad (3)$$

To solve this differential equation, we need to express D_{eff} as a function of X. For dynamic melting, the mass porosity (Φ) is defined as $\Phi = M_f/(M_f + M_s)$, where M_f is the mass of the residual melt and M_s is the mass of the residual solid. The effective distribution coefficient D_{eff} is related to the bulk distribution coefficient of the residual solid $D_{s/f}$ in the following way

$$D_{eff} = \Phi + (1 - \Phi) D_{s/f} \quad (4)$$

The mass conservation for phase i gives

$$M_0(1-F)x^i + M_0 F p^i = M_0 x_0^i \quad (5)$$

where p^i is the fractional contribution of phase i to the melt, x_0^i is the initial fraction of phase i in the source, $M_0(1-F)$ is the mass of the residual solid, and M_0F is the mass of the total melt (residual melt + extracted melt). Eqn. 5 may be rewritten as

$$x^i(F) = \frac{x_0^i - F p^i}{1 - F} \quad (6)$$

Similar to the methods used by Greenland (1970) for perfect fractional crystallization and those used by Hertogen and Gijbels (1976) for perfect fractional melting, we assume that the mineral/melt distribution coefficient K^i is a function of the degree of partial melting (F). Although the fundamental variables for K^i are temperatures, pressures, and chemical compositions, we choose F as the independent variable due to practical considerations to avoid too many unconstrained parameters. We then expand $K^i(F)$ in a Taylor series and only retain terms up to the first order

$$K^i(F) = K_0^i + a^i F \quad (7)$$

The above simple assumption of linear variation of $K^i(F)$ as a function of F is at least appropriate for evaluating the major effects of decreasing or increasing distribution coefficients (Greenland, 1970; Hertogen and Gijbel, 1976). More complicated forms of the distribution coefficients as a function of F can also be assumed; however, they involve more parameters and do not necessarily better describe the variations in distribution coefficients. A combination of Eqns. 1, 6, and 7 results in

$$D_{s/f} = \Sigma\, x^i(F) K^i(F) = \Sigma \frac{x_0^i - F p^i}{1 - F} (K_0^i + a^i F) \quad (8)$$

The following relationship between F and X, which is the fraction of the extracted melt relative to the initial solid, is necessary to express $D_{s/f}$ as a function of X (Zou, 1998)

$$F = \Phi + (1 - \Phi) X \quad (9)$$

Substituting Eqn. 9 into Eqn. 8, we obtain

$$D_{s/f} = \Sigma \frac{x_0^i - [\Phi + (1 - \Phi) X] p^i}{1 - [\Phi + (1 - \Phi) X]} \{K_0^i + a^i [\Phi + (1 - \Phi) X]\} \quad (10)$$

If $\Phi = 0$ and $a^i = 0$ for all i, which is the case for perfect fractional melting with constant mineral/melt distribution coefficients, Eqn. 10 reduces to the following equation of Shaw (1970): $D_{s/f} = (D_0 - P_0 F)/(1-F)$, where $D_0 = \Sigma x_0^i K_0^i$ is the initial bulk distribution coefficient and $P_0 = \Sigma p^i K_0^i$ is the weighted distribution coefficient of the total melt. Substituting Eqn. 10 into Eqn. 4, we finally express D_{eff} as a function of X

$$D_{eff} = \frac{1}{1 - X} (AX^2 + BX + Q) \quad (11)$$

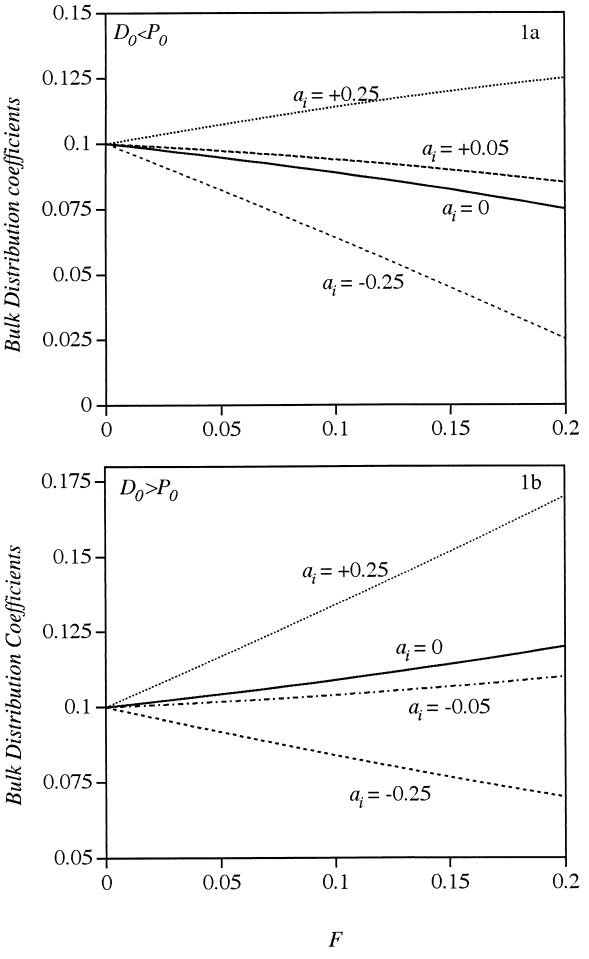

Fig. 1. Variations of bulk distribution coefficients ($D_{s/f}$) as a function of total melting degree (F) according to Eqn. 8 in the cases where $D_0 < P_0$ and where $D_0 > P_0$, respectively. For these hypothetical examples, it is assumed that $D_0 = 0.10$ and $P_0 = 0.20$ for the first case and $D_0 = 0.10$ and $P_0 = 0.02$ for the second case. The residual solid phases are assumed to have the same a_i for simplicity.

Table 1. The initial and the final mineral/melt partition coefficients for Nd, Yb, and Co.

		Constant K^i				Increasing K^i				Decreasing K^i			
		cpx	opx	ol	gt	cpx	opx	ol	gt	cpx	opx	ol	gt
Nd	$F = 0$	0.19	0.01	0.002	0.057	0.19	0.01	0.002	0.057	0.19	0.01	0.002	0.057
	$F = F_{max}$	0.19	0.01	0.002	0.057	0.38	0.02	0.004	0.114	0.095	0.005	0.001	0.0285
Yb	$F = 0$	0.50	0.075	0.059	7.0	0.50	0.075	0.059	7.0	0.50	0.075	0.059	7.0
	$F = F_{max}$	0.50	0.075	0.059	7.0	1.00	0.150	0.118	14.0	0.25	0.0375	0.0295	3.5
Co	$F = 0$	2.0	1.2	2.0	3.9	2.0	1.2	2.0	3.9	2.0	1.2	2.0	3.9
	$F = F_{max}$	2.0	1.2	2.0	3.9	4.0	2.4	4.0	7.8	1.0	0.6	1.0	1.95

Sources of distribution coefficients for constant K^i: Nd and Yb, Table A1 of Johnson et al. (1990); Co, Table A1 of Frey et al. (1978). In the calculation for Figures 2–4, the mineral compositions of the initial solid are $x_0^{cpx} = 0.15$, $x_0^{opx} = 0.20$, $x_0^{ol} = 0.55$, $x_0^{gt} = 0.10$ and the melting proportions are $p^{cpx} = 0.25$, $p^{opx} = 0.12$, $p^{ol} = 0.13$, $p^{gt} = 0.50$ (Johnson et al., 1990). Other parameters chosen: $F_{max} = 15\%$ and $\Phi = 0.1\%$. cpx = clinopyroxene, opx = orthopyroxene, ol = olivine, and gt = garnet. The final distribution coefficients are two times for increasing K^i and half for decreasing K^i as the initial values.

where

$$A = -(\Sigma a^i p^i)(1 - \Phi)^2 \tag{12}$$

$$B = -\Phi - (P_0 - \Sigma a^i x_0^i)(1 - \Phi) - 2\Phi(1 - \Phi)(\Sigma a^i p^i) \tag{13}$$

and

$$Q = \Phi + D_0 - \Phi(P_0 - \Sigma a^i x_0^i) - (\Sigma a^i p^i)\Phi^2 \tag{14}$$

A combination of Eqns. 3 and 11 gives us

$$\frac{d(X\overline{C_L})}{C_0 - X\overline{C_L}} = \frac{dX}{AX^2 + BX + Q} \tag{15}$$

When all $a^i = 0$, in other words, $A = 0$, then according to Eqns. 13 and 14, we obtain $B = -\Phi - P_0(1-\Phi)$ and $Q = D_0 + \Phi(1-P_0)$. Therefore, Eqn. 15 reduces to

$$\frac{d(X\overline{C_L})}{C_0 - X\overline{C_L}} = \frac{dX}{[-\Phi - P_0(1 - \Phi)]X + [D_0 + \Phi(1 - P_0)]} \tag{16}$$

The solution to Eqn. 16 is

$$\overline{C_L} = \frac{C_0}{X}\left\{1 - \left[1 - \frac{X[P_0 + \Phi(1 - P_0)]}{D_0 + \Phi(1 - P_0)}\right]^{1/[\Phi + (1-\Phi)P_0]}\right\} \tag{17}$$

which is Eqn. 34 in Zou (1998) for nonmodal dynamic melting with constant mineral/melt distribution coefficients obtained from a different approach.

When $A \neq 0$, the solutions to Eqn. 15 have the following three cases. If $\Delta = B^2 - 4AQ > 0$, then

$$\overline{C_L} = \frac{C_0}{X}\left\{1 - \left|\frac{(2AX + B + h)(B - h)}{(2AX + B - h)(B + h)}\right|^{\frac{1}{h}}\right\} \tag{18a}$$

$$C_f = \frac{d(X\overline{C_L})}{dX} = C_0 \frac{B - h}{B + h} \frac{4A}{(2AX + B - h)^2} \left|\frac{(2AX + B + h)(B - h)}{(2AX + B - h)(B + h)}\right|^{(1/h)-1} \tag{18b}$$

where

$$h = \sqrt{B^2 - 4AQ}; \tag{18c}$$

if $\Delta = 0$, then

$$\overline{C_L} = \frac{C_0}{X}\left[1 - \exp\left(\frac{2}{2AX + B} - \frac{2}{B}\right)\right] \tag{19a}$$

$$C_f = \frac{4AC_0}{(2AX + B)^2} \exp\left(\frac{2}{2AX + B} - \frac{2}{B}\right) \tag{19b}$$

and if $\Delta < 0$, then

$$\overline{C_L} = \frac{C_0}{X}\left\{1 - \exp\left[\frac{2}{k}\left(\arctan\frac{B}{k} - \arctan\frac{2AX + B}{k}\right)\right]\right\} \tag{20a}$$

$$C_f = \frac{4AC_0}{k^2} \frac{1}{1 + \left(\frac{2AX + B}{k}\right)^2} \exp\left[\frac{2}{k}\left(\arctan\frac{B}{k} - \arctan\frac{2AX + B}{k}\right)\right] \tag{20b}$$

where

$$k = \sqrt{4AQ - B^2}. \tag{20c}$$

For all the above three cases, the concentration in the residual solid is

$$C_s = D_{s/f} C_f \tag{21}$$

where $D_{s/f}$ is given by Eqn. 10, and the concentration for the total residue is

$$C_{res} = C_f\Phi + C_s(1 - \Phi) \tag{22}$$

It can be verified that all these solutions satisfy the mass balance requirement

$$\overline{C_L}X + C_{res}(1 - X) = C_0 \tag{23}$$

It is noted that Eqns. 18–20 for $\overline{C_L}$ and C_f are suitable for

dynamic melting when $F > \Phi$. In the case where $F \leq \Phi$, there is no melt extraction and the mass balance equation gives

$$C_f F M_0 + C_s(1 - F) M_0 = C_0 M_0 \quad (24)$$

or,

$$C_f = \frac{C_0}{F + D_{s/f}(1 - F)} \quad (25)$$

Substituting Eqn. 8 into Eqn. 24, we obtain

$$C_f = \frac{C_0}{F + \Sigma(x_0^i - Fp^i)(K_0^i + a^i F)} \quad (26)$$

or,

$$C_f = \frac{C_0}{D_0 + F(1 - P_0) + \Sigma a^i (x_0^i F - p^i F^2)} \quad (27)$$

as a result of $D_0 = \Sigma x_0^i K_0^i$ and $P_0 = \Sigma p^i K_0^i$. If $a^i = 0$ for all i, Eqn. 27 reduces to $C_f = C_0/[D_0 + F(1-P_0)]$, which is the well-known nonmodal batch melting Eqn. 15 of Shaw (1970) with constant mineral/melt distribution coefficients.

In summary, for nonmodal dynamic melting with linear variation of mineral/melt distribution coefficients, when $F \leq \Phi$, we use Eqn. 27; when $F > \Phi$, we choose Eqns. 18, 19, or 20, depending on the value of the discriminant Δ. For nonmodal dynamic melting with constant mineral/melt distribution coefficients ($a^i = 0$ and thus $A = 0$), we need to use the previously available equations (Pedersen and Hertogen, 1990; Sobolev and Shimizu, 1992; Zou, 1998).

3. DISCUSSION AND APPLICATIONS

3.1. Variations of Bulk Distribution Coefficients $D_{s/f}$

If we consider the variation in x^i while keeping K^i fixed, the bulk distribution coefficient has been given by Shaw (1970) as $D_{s/f} = (D_0 - P_0F)(1-F)$. Consequently, we have $d(D_{s/f})/dF = (D_0 - P_0)/(1-F)^2$. If $D_0 < P_0$, then $d(D_{s/f})/dF < 0$ and $D_{s/f}$ decreases as melting proceeds (Fig. 1a); and if $D_0 > P_0$, then $d(D_{s/f})/dF > 0$ and $D_{s/f}$ increases during melting (Fig. 1b). In fact, the relationship $D_0 < P_0$ implies the preferential melting of the minerals with high mineral/melt distribution coefficients and thus the solid residue is left with higher proportions of minerals of low distribution coefficients; the opposite is true for the case where $D_0 > P_0$.

If we consider the variations in both x^i and K^i, the change of $D_{s/f}$ is more complex, and the effects of the mineral proportions and the mineral/melt distribution coefficients on the bulk distribution coefficient may be similar or opposite. When $D_0 < P_0$ (Fig. 1a), if mineral/melt distribution coefficients are decreasing ($a^i < 0$), $D_{s/f}$ decreases even faster than traditional nonmodal melting model ($a^i = 0$); if $a^i > 0$, the preferential melting of the minerals with high distribution coefficients tends to decrease $D_{s/f}$, whereas the increase of individual mineral distribution coefficients tends to increase $D_{s/f}$. The net result of the two opposite effects will determine the actual variation of $D_{s/f}$ (Fig. 1a). Consequently, it is important to realize that, for the case where $D_0 < P_0$, even though the minerals with high distribution coefficients preferentially enter the melt during partial melting, there is a possibility that the bulk distribution coefficient of an element may increase due to the possible increase of mineral/melt distribution coefficients. Similarly, for the case where $D_0 > P_0$ (Fig. 1b), even though the minerals with low distribution coefficients enter the melt preferentially, there is a chance that the bulk distribution coefficient may decrease as a result of the decreasing mineral/melt distribution coefficients. As far as mantle melting in the spinel stability field is concerned, available experiments have indicated $D_0 < P_0$ and $a^{cpx} < 0$ for Ti and Lu (Baker et al., 1995; Blundy et al., 1998).

3.2. Effects of Varying Mineral/Melt Distribution Coefficients

We select three trace elements with different levels of bulk distribution coefficients, Nd (an incompatible element), Yb (a not-so-incompatible element), and Co (a compatible element). We will compare the effects of variable mineral/melt distribution coefficients on trace element fractionation by studying the following three cases:

1. the mineral/melt distribution coefficients of all three elements gradually increase to two folds at the maximum degree of partial melting;
2. the mineral/melt distribution coefficients remain constant; and
3. the mineral/melt distribution coefficients of all three elements gradually decrease to half of their initial values at the maximum degree of melting.

The related modeling parameters are listed in Table 1 and an example of step-by-step calculation for Nd with $X = 5\%$ is given in Appendix B.

The effects of mineral/melt distribution coefficient variations on trace element fractionation in general vary with elements and subsystems (the extracted melt, the residual melt, and the residual solid). For Nd, the effects of varying mineral/melt distribution coefficients are small for both the extracted melt (Fig. 2a) and the residual melt (Fig. 2b) but are noted for the residual solid (Fig. 2c).

For Yb, the effects are significant for the extracted melt (Fig. 3a), the residual melt (Fig. 3b), and the residual solid (Fig. 3c), particularly at high degrees of melting.

As for Co, the effects are marked for both the extracted melt (Fig. 4a) and the residual melt (Fig. 4b), particularly at high degrees of melting. But the effects are very small for the residual solid (Fig. 4c).

It is noted that there are cases where the distribution coefficients in some minerals increase while those in other minerals decrease with the degree of partial melting. The net result is to reduce the effect of variable K^i. Also note that mineral/melt distribution coefficients may decrease by a factor of four during melting (e.g., Baker et al., 1995; Blundy et al., 1998), which can magnify the effect of variable K^i.

3.3. Geochemical Applications

There are only a few experimental studies on the changes of mineral/melt distribution coefficients as a function of F. Available data have showed nearly linear variations in cpx/melt distribution coefficients for Ti and Lu with F (Baker et al.,

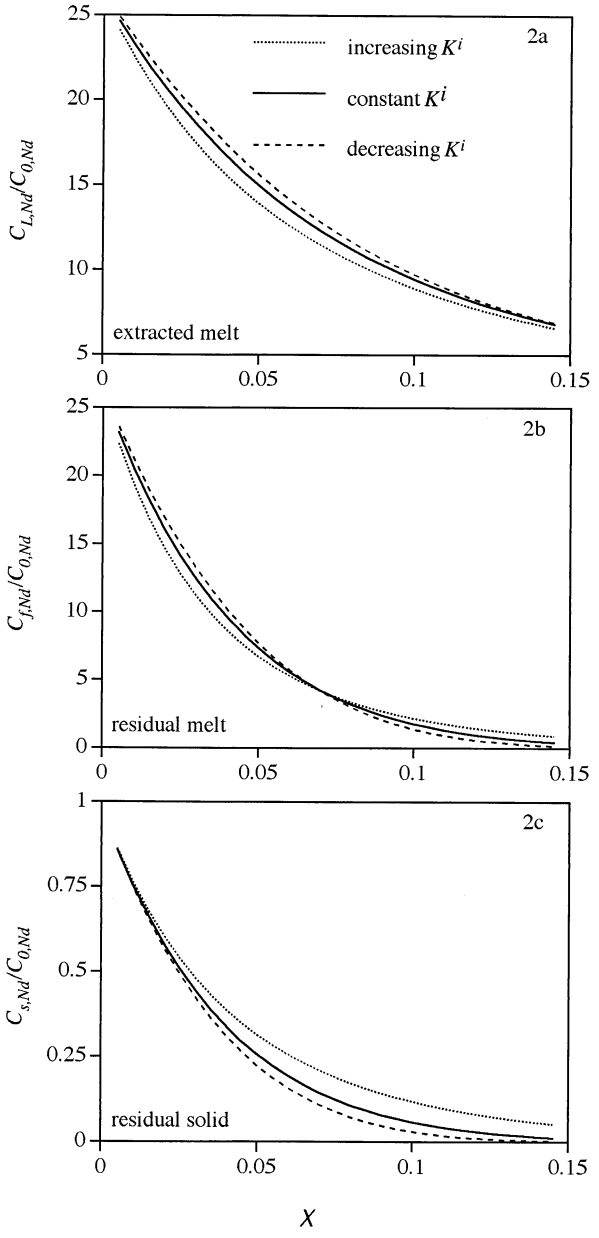

Fig. 2. The concentrations of Nd normalized to its initial source concentration in the extracted melt, the residual melt, and the residual solid, produced by nonmodal dynamic melting of a garnet peridotite source with constant K^i, increasing K^i, and decreasing K^i, respectively. The related parameters are given in Table 1.

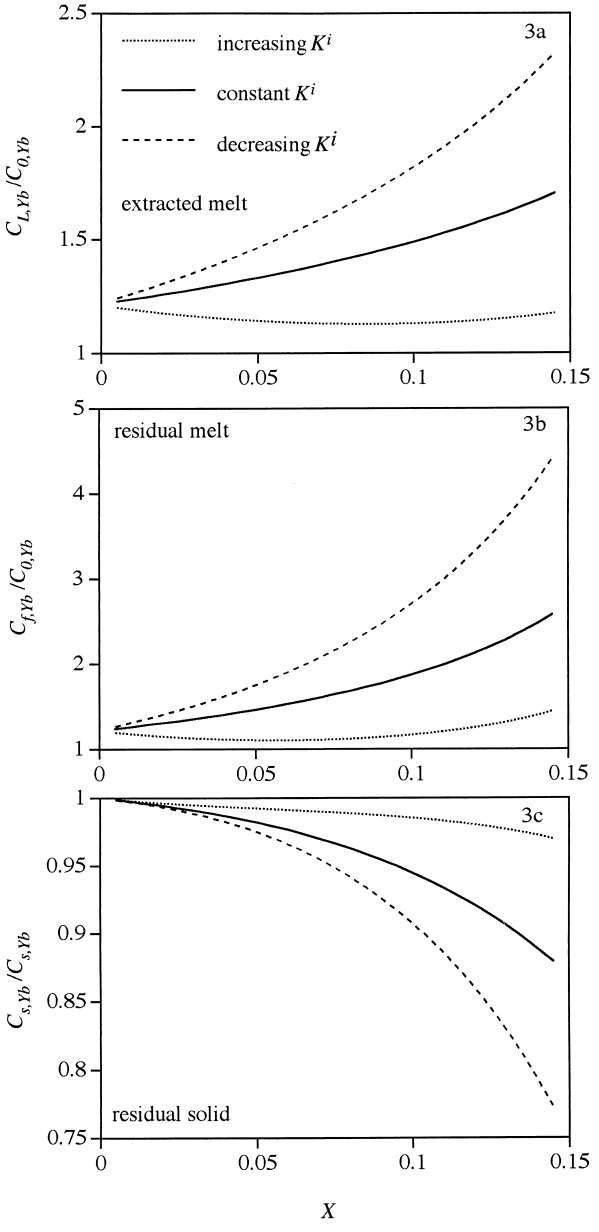

Fig. 3. The concentrations of Yb normalized to its initial source concentration in the extracted melt, the residual melt, and the residual solid, respectively, produced by nonmodal dynamic melting of a garnet peridotite source with constant K^i, increasing K^i, and decreasing K^i, respectively. The related parameters are given in Table 1.

1995; Blundy et al., 1998). Based on Fig. 2c of Baker et al. (1995), we obtain $K_0^{cpx} = 0.60$ and $a^{cpx} = -4.0$ for Ti when $F \leq 0.10$. Similarly, according to Figure 5 of Blundy et al. (1998), we have $K_0^{cpx} = 1.75$ and $a^{cpx} = -11.5$ for Lu when $F \leq 0.10$. Conventional models of mantle melting in spinel-stability field generally use constant K^{cpx} obtained at high degrees of melting. By taking account of high but varying K^{cpx} at low degrees of melting, the equations here can yield quite different results for Lu to the conventional constant K^{cpx} models (Fig. 5a–5c). For example, when X increases from 0.0025 to 0.10, the calculated source-normalized Lu concentrations in the extracted melt from spinel peridotite mantle change from 3.1 to 4.6 using the equations here but vary from 10.8 to 7.3 according to the constant K^{cpx} dynamic melting model. Compared with the constant K^{cpx} model, the low Lu concentrations in the extracted melt calculated from variable K^{cpx} model for spinel peridotitie melting are much closer to the results for melting of slightly depleted garnet peridotites (Fig. 5a). Due to the more garnet-like behavior of clinopyroxene at low degrees of melting (Blundy et al., 1998), modeling using the equations here can reduce the required involvement of garnet in the melting region beneath mid-ocean ridges (Salters and Hart, 1989; Salters, 1996).

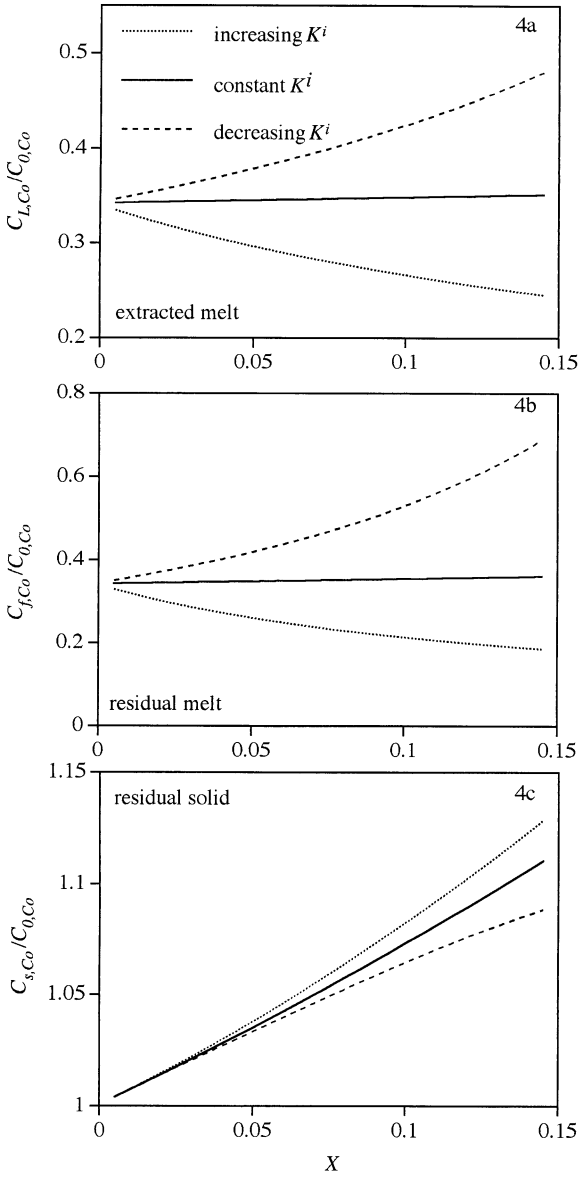

Fig. 4. The concentrations of Co normalized to its initial source concentration in the extracted melt, the residual melt, and the residual solid, produced by nonmodal dynamic melting of a garnet peridotite source with constant K^i, increasing K^i, and decreasing K^i, respectively. The related parameters are given in Table 1.

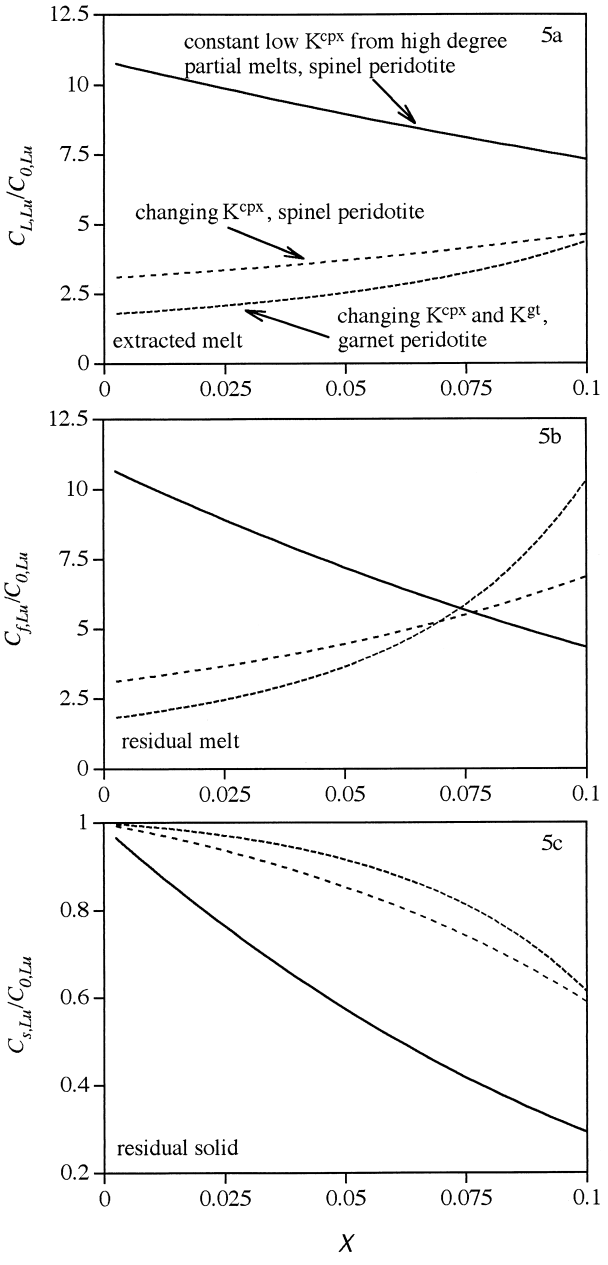

Fig. 5. The source normalized Lu concentrations in the extracted melt, the residual melt, and the residual solid, respectively, produced by nonmodal dynamic melting of a spinel peridotite source with constant K^{cpx} and decreasing K^{cpx}, respectively. Even for the case with decreasing K^{cpx}, the distribution coefficients for other minerals (ol, opx, and sp) are assumed constant. The source-normalized Lu concentrations produced by nonmodal dynamic melting of a slightly depleted garnet peridotite source with decreasing K^{cpx} and K^{gt} are also calculated for comparison. The composition of the spinel peridotites is 0.55 ol + 0.25 opx + 0.18 cpx + 0.02 sp and the melting mode is 0.10 ol + 0.20 opx + 0.68 cpx + 0.02 sp (Johnson et al., 1990). The composition of the slightly depleted garnet peridotites is 0.66 ol + 0.20 opx + 0.08 cpx + 0.06 gt (Maaløe and Aoki, 1977) and the melting mode is 0.03 ol + 0.03 opx + 0.44 cpx + 0.50 gt (Johnson et al., 1990). Distribution coefficients for Lu are $K_0^{ol} = 0.0048$, $K_0^{opx} = 0.038$, $K_0^{gt} = 7$ (set 1 by Frey et al., 1978), and $K_0^{cpx} = 1.75$ (Blundy et al., 1998). Other parameters chosen: $a^{cpx} = -11.5$ and $a^{gt} = -46.6$, and $\Phi = 0.1\%$.

If the dramatic changes of K^{cpx} in near-solidus melting for Ti and Lu are general for other elements and mineral-melt couples, then we must be more careful in the interpretation of trace element patterns in basalts, melt inclusions, and residual clinopyroxenes and peridotites. Certain elemental ratios (e.g., K_2O/TiO_2) thought to be constant during melting may, in fact, vary for low-degree partial melts (Baker et al., 1995). Therefore, the changes in distribution coefficients must be more carefully assessed in the practice of using some elemental ratios to characterize mantle source compositions. Clearly, comprehensive applications of the equations here to better understand-

ing of trace element fractionation during melting require much more experimental data on trace element partitioning.

Eqns. 18–20 are valid for linear variations (i.e., constant a^i) of mineral/melt distribution coefficients. It is possible that a^i may change as melting proceeds. For example, Figure 2 of Baker et al. (1995) and Figure 5 of Blundy et al. (1998) show that experimentally-determined K^{cpx} for Ti and Lu falls rapidly with increasing F when $F \leq 10\%$ and very slowly when $F > 10\%$. This suggests a large negative a^{cpx} (i.e., the slope in K^{cpx} vs. F diagram) for $F \leqq 10\%$ and a small negative a^{cpx} for $F > 10\%$. In this case, the trace element concentrations for high-degree melts ($F > 10\%$) can be calculated from step-wise numerical methods by simply applying the calculation here to an approach that uses a different a^i for each of the two melting intervals.

To sum up, this paper provides solutions for the nonmodal dynamic melting model with varying mineral/melt distribution coefficients and evaluates the effects of the mineral/melt distribution coefficient variations on trace element fractionation. In general, for the same percentage of distribution coefficient variations, the effects will be more significant for not-so-incompatible elements (e.g., Yb) in all subsystems and for compatible elements in the extracted melt and the residual melt, particularly at high degrees of melting. On the other hand, the incompatible element fractionation in the extracted melt and the residual melt is not very sensitive to the distribution coefficient variations. Modeling using varying distribution coefficients can reduce the required involvement of garnet in the generation of mid-ocean ridge basalts. When using trace element concentrations or ratios to study the petrogenesis of igneous rocks and their inclusions, we need to carefully evaluate the effects of changing mineral/melt distribution coefficients for the related trace elements. More experimental data on trace element partitioning, particularly at low degrees of melting, are needed in order to apply the equations here to a wide range of geochemical studies.

Acknowledgments—I am grateful to Drs. Paul Asimow and Yan Liang for their constructive reviews that significantly improved the quality of this paper. Dr. Jon Blundy provided useful suggestions and references for trace element partitioning. I also thank Dr. Karl Turekian for his speedy handing of this manuscript. This work was supported by a National Science Foundation Earth Sciences Postdoctoral Research Fellowship Award (EAR 98-05687) to the author.

REFERENCES

Albarède F. (1995) Introduction to Geochemical Modeling. Cambridge Univ. Press.

Baker M. B., Hirschman M. M., Ghiorso M. S., and Stolper E. M. (1995) Compositions of near-solidus peridoite melts from experiments and thermodynamic calculations. *Nature* **375,** 308–311.

Beattie P. (1993) Uranium-thorium disequilibria and partitioning of melt of garnet peridotite. *Nature* **363,** 63–65.

Blundy J. D., Robinson J. A. C., and Wood B. J. (1998) Heavy REE are compatible in clinopyroxene on the spinel lherzolite solidus. *Earth Planet. Sci. Lett.* **160,** 493–504.

Chabaux F. and Allègre C. J. (1994) ^{238}U-^{230}Th-^{226}Ra disequilibria in volcanics: A new insight into melting conditions. *Earth Planet. Sci. Lett.* **126,** 61–74.

Frey F. A., Green D. H., and Roy S. D. (1978) Integrated models of basalts petrogenesis: A study of quartz tholeiite to olivine melilitites from South Eastern Australia utilizing geochemical and experimental data. *J. Petrol.* **19,** 463–513.

Greenland L. P. (1970) An equation for trace element distribution during magmatic crystallization. *Am. Mineral.* **55,** 455–465.

Gurenko A. A. and Chaussidon M. (1995) Enriched and depleted primitive melts included in olivine from Icelandic tholeiites: Origin by continuous melting of a single mantle column. *Geochim. Cosmochim. Acta* **59,** 2905–2917.

Hertogen J. and Gijbels R. (1976) Calculation of trace element fractionation during partial melting. *Geochim. Cosmochim. Acta* **40,** 313–322.

Johnson K. T. M., Dick H. J. B., and Shimizu N. (1990) Melting of the oceanic upper mantle: An ion microprobe study of diopsides in abyssal peridotites. *J. Geophys. Res.* **95,** 2661–2678.

Langmuir C. H., Bender J. F., Bence A. E., Hanson G. N., and Taylor S. R. (1977) Petrogenesis of basalts from the FAMOUS-area, Mid-Atlantic ridge *Earth Planet. Sci. Lett.* **36,** 133–156.

Maaløe S. (1982) Geochemical aspects of permeability-controlled partial melting and fractional crystallization. *Geochim. Cosmochim. Acta* **46,** 43–57.

Maaløe S. and Aoki K. (1977) The major element composition of the upper mantle estimated from the composition of lherzolites. *Contrib. Mineral. Petrol.* **93,** 449–458.

Maaløe S. and Johnson D. (1986) Geochemical aspects of some accumulation models for primary magmas. *Contrib. Mineral. Petrol.* **93,** 449–458.

McKenzie D. P. (1985) ^{230}Th-^{238}U disequilibrium and the melting processes beneath ridge axes. *Earth Planet. Sci. Lett.* **72,** 149–157.

Ozawa K. and Shimizu N. (1995) Open-system melting in the upper mantle: Constraints from the Hayachine-Miyamori ophiolite, northeastern Japan. *J. Geophys. Res.* **100,** 22315–22335.

Pedersen R. B. and Hertogen J. (1990) Magmatic evolution of the Karmoy Ophiolite Complex, SW Norway: relationship between MORB-IAT-boninitic-calc-alkaline and alkaline magmatism. *Contrib. Mineral. Petrol.* **104,** 277–293.

Ross K. and Elthon D. (1993) Cumulates from strongly depleted mid-ocean-ridge basalt. *Nature* **365,** 826–829.

Salters V. J. M. (1996) The generation of mid-ocean ridge basalts from the Hf and Nd perspective. *Earth Planet. Sci. Lett.* **141,** 109–123.

Salters V. J. M. and Hart S. R. (1989) The hafnium paradox and the role of garnet in the source of mid-ocean ridge basalts. *Nature* **342,** 420–422.

Shaw D. M. (1970) Trace element fractionation during anatexis. *Geochim. Cosmochim. Acta* **34,** 237–243.

Shimizu N. (1998) The geochemistry of olivine-hosted melt inclusions in FAMOUS basalts ALV519–4-1. *Phys. Earth Planet. Int.* **107,** 183–201.

Sobolev A. V. and Shimizu N. (1992) Superdepleted melts and ocean mantle permeability. *Doklady Rossiyskoy Akademii Nauk* **326,** 354–360.

Sobolev A. V. and Shimizu N. (1993) Ultra-depleted primary melt included in an olivine from the Mid-Atlantic Ridge. *Nature* **363,** 151–154.

Williams R. W. and Gill J. B. (1989) Effect of partial melting on the uranium decay series. *Geochim. Cosmochim. Acta* **53,** 1607–1619.

Zou H. (1998) Trace element fractionation during modal and nonmodal dynamic melting and open-system melting: A mathematical treatment. *Geochim. Cosmochim. Acta* **62,** 1937–1945.

Zou H. and Zindler A. (1996) Constraints on the degree of dynamic partial melting and source composition using concentration ratios in magma. *Geochim. Cosmochim. Acta* **60,** 711–717.

APPENDIX A: NOTATIONS

M_0	the total mass of the initial solid
M_L, M_f, M_s	the mass of the extracted melt, the residual melt, and the residual solid, respectively
m_0	the total mass of an element in the initial solid
m_L, m_f, m_s	the mass of an element in the extracted melt, the residual melt, and the residual solid, respectively
C_0	m_0/M_0, the concentration of an element in the initial solid source
$\overline{C_L}$	m_L/M_L, the concentration of an element in the extracted melt
C_f	m_f/M_f, the concentration of an element in the residual melt
C_s	m_s/M_s, the concentration of an element in the residual solid
C_{res}	$= (m_f + m_s)/(M_f + M_s)$, the concentration of an element in the total residue
F	$= (M_f + M_L)/M_0$, the total degree of partial melting, i.e., the fraction of the initial solid that is converted into melt (residual melt and extracted melt)
X	$= M_L/M_0$, the fraction of extracted melt relative to the initial solid
p^i	the fractional contribution of phase i to the melt
x_0^i	the mass fraction of phase i in the initial solid
x^i	the mass fraction of phase i in the solid during melting
K_0^i	the mineral/melt distribution coefficient for phase i in the initial solid
K^i	the mineral/melt distribution coefficient for phase i during melting
D_0	$= \Sigma\, x_0^i\, K_0^i$, the initial bulk distribution coefficient
P_0	$= \Sigma\, p^i\, K_0^i$, the weighted distribution coefficient of the melt
$D_{s/f}$	the bulk solid/melt distribution coefficient during melting
D_{eff}	the effective distribution coefficient defined in Eqn. 3
Φ	the critical mass porosity
a^i	the variation rate of distribution coefficient for phase i defined in Eqn. 7

APPENDIX B: AN EXAMPLE

The following example is a step-by-step calculation of the source-normalized Nd concentration in all subsystems for the case of increasing K^i with $X = 5\%$. The related parameters are from Table 1.

(1) Calculation of a^i

Given $F_{\max} = 0.15$, according to Eqn. 7, we have (AP1)

$a^{cpx} = (K_{\max}^{cpx} - K_0^{cpx})/F_{max} = (0.38 - 0.19)/0.15 = 1.267$

Similarly, $a^{opx} = 0.067$, $a^{ol} = 0.013$, and $a^{gt} = 0.380$.

(2) Calculation of D_0, P_0, $\Sigma\, a^i\, x_0^i$, and $\Sigma a^i\, p^i$

$$D_0 = \Sigma\, x_0^i K_0^i = x_0^{cpx} K_0^{cpx} + x_0^{opx} K_0^{opx} + x_0^{ol} K_0^{ol} + x_0^{gt} K_0^{gt}$$
$$= 0.15 \times 0.19 + 0.20 \times 0.01 + 0.55 \times 0.002 + 0.10 \times 0.057$$
$$= 0.0373 \quad \text{(AP2)}$$

$$P_0 = \Sigma\, p^i K_0^i = p^{cpx} K_0^{cpx} + p^{opx} K_0^{opx} + p^{ol} K_0^{ol} + p^{gt} K_0^{gt}$$
$$= 0.25 \times 0.19 + 0.12 \times 0.01 + 0.13 \times 0.002 + 0.50 \times 0.057$$
$$= 0.0775 \quad \text{(AP3)}$$

$$\Sigma\, a^i x_0^i = a^{cpx} x_0^{cpx} + a^{opx} x_0^{opx} + a^{ol} x_0^{ol} + a^{gt} x_0^{gt}$$
$$= 1.267 \times 0.15 + 0.067 \times 0.20 + 0.013 \times 0.55 + 0.380 \times 0.10 = 0.2486 \quad \text{(AP4)}$$

$$\Sigma\, a^i p^i = a^{cpx} p^{cpx} + a^{opx} p^{opx} + a^{ol} p^{ol} + a^{gt} p^{gt}$$
$$= 1.267 \times 0.25 + 0.067 \times 0.12 + 0.013 \times 0.13 + 0.38 \times 0.50 = 0.5165 \quad \text{(AP5)}$$

(3) Calculation of A, B, Q, and Δ

$$A = -0.5165 \times (1 - 0.001)^2 = -0.5155$$
$$B = -0.001 - (0.0775 - 0.2486)(1 - 0.001) - 2 \times 0.001 \times (1 - 0.001) \times 0.5165 = 0.1689$$
$$Q = 0.001 + 0.0373 - 0.001 \times (0.0775 - 0.2486) - 0.5165 \times 0.001^2 = 0.0385$$
$$\Delta = 0.1689^2 - 4 \times (-0.5155) \times 0.0385 = 0.1079$$

Since $\Delta > 0$, we will choose Eqn. 18 to calculate concentrations in step (4).

(4) Calculation of the concentrations in all subsystems

$$h = \sqrt{B^2 - 4AQ} = 0.3285. \quad \text{(AP6)}$$

Substituting all parameters into Eqns. 18a and 18b, we obtain

$$\overline{C_L^{Nd}}/C_0^{Nd} = 13.886 \quad \text{(AP7)}$$

$$C_f^{Nd}/D_0^{Nd} = 6.696 \quad \text{(AP7a)}$$

According to Eqn. 11,

$$D_{eff} = 0.04806$$

Based on Eqn. 3,

$$D_{s/f} = 0.0471$$

From Eqns. 21 and 22, we have

$$C_s^{Nd}/C_0^{Nd} = 0.3154 \quad \text{(AP8)}$$

$$C_{res}^{Nd}/C_0^{Nd} = 0.3218 \quad \text{(AP8a)}$$

It can be verified that, for $X = 0.05$, the solutions satisfy Eqn. 23 for the mass balance requirement,

$$X\overline{C_L}/C_0^{Nd} + (1 - X) C_{res}^{Nd}/C_0^{Nd} = 0.05 \times 13.886 + (1 - 0.05) \times 0.3218 = 1 \quad \text{(AP9)}$$